Journal of Advanced Scientific Research

Available online through https://sciensage.info

ISSN

0976-9595

Research Article

TUNABLE OPTICAL AND STRUCTURAL PROPERTIES OF NITROGEN AND COBALT CO-DOPED CDS NANOPARTICLES FOR OPTOELECTRONIC APPLICATIONS

M. Surya Sekhar Reddy

Department of Physics, SVCR Government Degree College, Palamaner. A.P. India. 517408

*Corresponding author: msrphd2022@gmail.com

Received: 08-10-2022; Accepted: 10-11-2022; Published: 31-12-2022

© Creative Commons Attribution-NonCommercial-NoDerivatives 4.0 International License

https://doi.org/10.55218/JASR.2022131113

ABSTRACT

Cadmium sulfide, a II-VI semiconductor with a wide band gap, is a promising material for applications in spintronics, optoelectronics, and next-generation smart devices. This study investigates the synthesis, structural, and optical properties of nitrogen (N) and cobalt (Co) co-doped CdS and $Cd_{0.96-x}Co_{0.04}N_xS$ nanoparticles (where x = 0, 0.02, 0.04, 0.06, and 0.08) prepared via a co-precipitation method at room temperature. X-ray diffraction and Rietveld refinement confirmed the formation of mixed cubic and hexagonal phases, with doping-induced lattice strain and nano crystallinity. Fourier transform infrared spectra revealed characteristic bonding features and the role of Co and N in stabilising the nanoparticles. UV-VIS analysis demonstrated tunable band gap energies, influenced by the Burstein-Moss effect and quantum confinement, ranging from 2.39 eV to 2.71 eV. The study highlights that Co and N doping enhances the optical and structural properties of CdS, making it suitable for optoelectronic technologies.

Keywords: CdS, Optoelectronic devices, Diluted magnetic semiconductors, Nanoparticles, Co-precipitation method

INTRODUCTION

Cadmium sulfide (CdS), a II-VI semiconductor, is recognised for its wide band gap, making it highly suitable for applications in light-emitting diodes, photocatalytic devices, address decoders, heterojunction solar cells, biological sensors, and gas detectors. The band gap can be readily tuned by introducing minor quantities of cationic or anionic impurities. Extensive research has focused on introducing cation metallic impurities to modify the optical, electrical, magnetic, and structural properties of CdS [1], [2-3]. Transition metal doping in CdS leads to the formation of diluted magnetic semiconductors (DMS), which are crucial in spintronic technologies where both spin and charge are manipulated to control device properties [4-5]. Beyond magnetic characteristics, the optical, electrical, and structural properties of doped CdS have garnered significant interest in developing next-generation smart devices. Various transition metals, including Cu, Zn, Cr, Mn, Fe, Co, and Ni, have been employed as dopants or co-dopants in CdS nanoparticles through various synthesis techniques [1], [6-11].

Among these, cobalt (Co) ions, with a radius of 79 pm, readily replace cadmium (Cd) ions of radius 109 pm in the CdS lattice. Researchers have synthesised and examined co-doped CdS, including co-doping with other transition elements, revealing notable optical, magnetic, and structural properties. However, recent studies indicate that the stability of these nanoparticles remains a challenge. To enhance their stability and fluorescence characteristics, elements like oxygen (O), selenium (Se), tellurium (Te), and nitrogen (N) have been identified as essential substitutional elements. Nitrogen, in particular, shows promise due to its high electronegativity and capacity to exist in multiple ionic states i.e. N^{3-}, N^{3+}, and N^{5+}, which can facilitate the formation of secondary compounds in CdS nanoparticles.

While several studies have investigated cationic (metallic) substitutions in CdS, there is limited research on non-metallic cationic substitutions. Nitrogen's potential to act as both an anionic and cationic substitute in CdS, unlike chalcogens and halogens, offers a new avenue for study. Recent work, such as nitrogen doping in ZnS and the stabilisation of CdS nanostructures through nitrogen inclusion, supports the potential of this approach [12]. The co-precipitation method, a simple and effective technique, is frequently used to prepare nanoparticles due to its low material requirements, scalability, and control over particle size. In this study, we successfully synthesised nitrogen and cobalt co-doped CdS nanoparticles at room temperature utilising a co-precipitation technique, with 2-mercaptoethanol as the capping agent.

The results reveal notable alterations in optical, electrical, mechanical, magnetic, and structural properties. These include ferromagnetic behaviour at low fields and adjustable band gap variations. Such findings emphasise the potential use of these nanoparticles in spintronic and opto-magnetic technologies.

Synthesis

CdS and $Cd_{0.94-x}Co_{0.04}N_xS$ nanoparticles (where x = 0, 0.02, 0.04, 0.06, and 0.08) were prepared using a chemical co-precipitation method with 99.9% purity chemicals sourced from Sigma Aldrich. Na_2S was an anionic precursor, while cadmium acetate dihydrate cobalt acetate tetrahydrate and thiourea were the cationic precursors. This synthesis approach facilitated the examination of the nanoparticles' optical, electrical, and structural properties. Similar methodologies have been employed in previous studies to prepare CdS and Co co-doped CdS nanoparticles, yielding insights into their structural and optical characteristics [13-14]

RESULTS AND DISCUSSION

Structural analysis

XRD analysis

The XRD patterns of CdS and $Cd_{0.96-x}Co_{0.04}N_xS$ nanoparticles (where x = 0, 0.02, 0.04, 0.06, and 0.08) are presented in Fig. 1. Three broad diffraction peaks were observed, corresponding to the cubic zinc blende (JCPDS 10-454) and hexagonal wurtzite (JCPDS card No. 41-1049) phases for pure CdS and doped $Cd_{0.96-x}Co_{0.04}N_xS$. For lower doping concentrations (x = 0, 0.02, and 0.04), the mixed cubic and hexagonal phases were predominant. The observed broadening of the peaks indicates the presence of nano crystallinity and strain. At higher doping concentrations (x = 0.06 and 0.08), low-intensity peaks at a 2θ angle of 43.7° were detected, corresponding to the Co_3N_2 phase (JCPDS card No. 10-178).

The summary of Co and N in the CdS lattice resulted in peak shifts towards higher 2θ values, suggesting a reduction in crystallite size with increased doping concentrations of N. This is attributed to the substitutional incorporation of Co^{2+} and N ions into the CdS lattice, causing lattice contraction. The crystallite sizes were calculated using the Debye-Scherrer formula [15] are presented in Table 1 and range from 1.57 nm to 2.01 nm.

Rietveld refinement

The Rietveld refinement was employed to achieve a more accurate determination of lattice parameters, crystallite size, and strain. Fig. 1 shows the calculated (blue) and observed (red) XRD profiles, with good agreement between the two, indicating the reliability of the refinement. The refinement confirmed the coexistence of cubic and hexagonal phases in the $Cd_{0.96-x}Co_{0.04}N_xS$ nanoparticles (where x = 0, 0.02, 0.04, 0.06, and 0.08) samples, with a notable increase in lattice strain for higher doping concentrations.

As shown in Table 1, the strain values calculated from the Rietveld analysis indicate a significant decrease for doped samples compared to pure CdS. This reduction in strain suggests a more stable crystalline structure with Co and N doping. Moreover, the shift in peak positions and the broadening of peaks with increasing N content support forming a solid solution due to Co and N incorporation into the CdS lattice. The Rietveld analysis confirmed the formation of a stable crystalline structure with reduced strain for doped samples [16]. These findings suggest that Co and N doping can effectively tune the structural properties of CdS nanoparticles for potential optoelectronic applications.

Optical studies

FTIR analysis

Figure 2 presents the Fourier transform infrared (FTIR) spectra obtained using the disc method for the synthesised CdS, and $Cd_{0.96-x}Co_{0.04}N_xS$ nanoparticles (where x = 0, 0.02, 0.04, 0.06, and 0.08).

Notable absorption peaks appear at 1452 cm^{-1} and 622 cm^{-1}, corresponding to Cd-S bond stretching [2], [17]. The peak at 563 cm^{-1}, observed at a lower frequency, suggests the presence of Co-N bonds. Additional peaks at 3250 cm^{-1} indicate O-H bond stretching, with related peaks appearing at 830 cm^{-1} and 1640 cm^{-1}. Peaks at 1005 cm^{-1} and 1044 cm^{-1} are linked to C-C bonding, while the $-CH_2$ group is identified by peaks at 2922 cm^{-1}, and C-S bonding is reflected at 654 cm^{-1} [18].

Overall, these results show a reduction in stretching frequencies, confirming the presence of Co^{2+} ions, nitrogen, and 2-mercaptoethanol, which functions as a surfactant to control nanoparticle size. This suggests the formation of additional compounds, as seen in X-ray diffraction Rietveld analysis, and highlights enhanced bonding energies. The incorporation of nitrogen and cobalt contributes to the stabilisation of the nanoparticles by increasing bonding energy.

UV-VIS absorption spectra

UV-VIS absorption spectra of the synthesised CdS, and $Cd_{0.96-x}Co_{0.04}N_xS$ nanoparticles (where x = 0, 0.02, 0.04, 0.06, and 0.08) are shown in Fig. 3.

UV-VIS absorption spectra provide valuable insights into the optical properties of synthesized nanoparticles. The absorption peak observed at 750 nm in the spectra confirms the successful incorporation of Co^{2+} ions into the CdS lattice. This characteristic peak is associated with the d-d electronic transitions of cobalt ions in the CdS host matrix, which indicates the substitution of Cd^{2+} by

Table 1: The crystallite size and lattice strain values of CdS and $Cd_{0.96-x}Co_{0.04}N_xS$ nanoparticles (where x = 0, 0.02, 0.04, 0.06, and 0.08).

Compound	*Crystallite size (nm)*	*Lattice strain*
CdS	1.08	0.140
$Cd_{0.96}Co_{0.04}S$	1.57	0.099
$Cd_{0.94}Co_{0.04}N_{0.02}S$	1.70	0.092
$Cd_{0.92}Co_{0.04}N_{0.04}S$	1.80	0.089
$Cd_{0.90}Co_{0.04}N_{0.06}S$	1.90	0.081
$Cd_{0.88}Co_{0.04}N_{0.08}S$	2.01	0.078

Table 2: The Band edge position and Band gap of CdS and $Cd_{0.96-x}Co_{0.04}N_xS$ nanoparticles (where x = 0, 0.02, 0.04, 0.06, and 0.08).

Compound	*Band edge position (nm)*	*Band gap (eV)*
CdS	540	2.55
$Cd_{0.96}Co_{0.04}S$	490	2.70
$Cd_{0.94}Co_{0.04}N_{0.02}S$	476	2.71
$Cd_{0.92}Co_{0.04}N_{0.04}S$	508	2.57
$Cd_{0.90}Co_{0.04}N_{0.06}S$	529	2.44
$Cd_{0.88}Co_{0.04}N_{0.08}S$	520	2.39

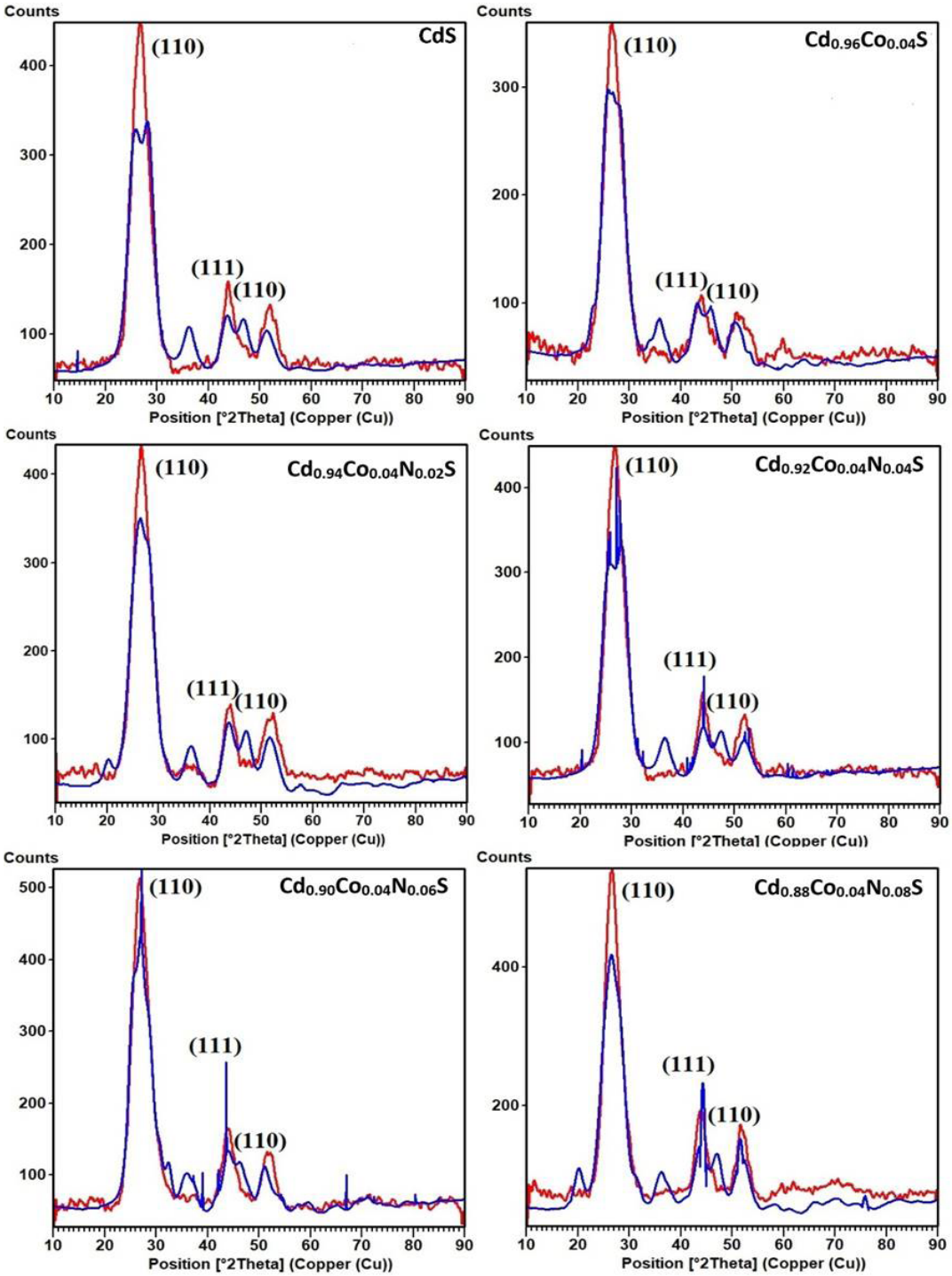


Fig. 1: The XRD patterns of CdS and $Cd_{1-x}Co_{0.04}N_xS$ nanoparticles (where x = 0, 0.02, 0.04, 0.06, and 0.08).

Co^{2+} in the lattice [18].

UV-VIS absorption band edge position

The absorption band edge positions of the synthesised nanoparticles, as derived from the absorption spectra, are illustrated in Fig. 4.

The spectra for CdS and $Cd_{0.96-x}Co_{0.04}N_xS$ nanoparticles (where x = 0, 0.02, 0.04, 0.06, and 0.08) reveal the band edge positions shown in Table 2. It is evident from the table that the absorption band edges initially shift towards shorter wavelengths, followed by a shift towards longer wavelengths as the N concentration in the doped samples increases. This observed redshift in the band edge suggests a narrowing of the band gap, reflecting changes in the electronic structure due to the dopant incorporation [2].

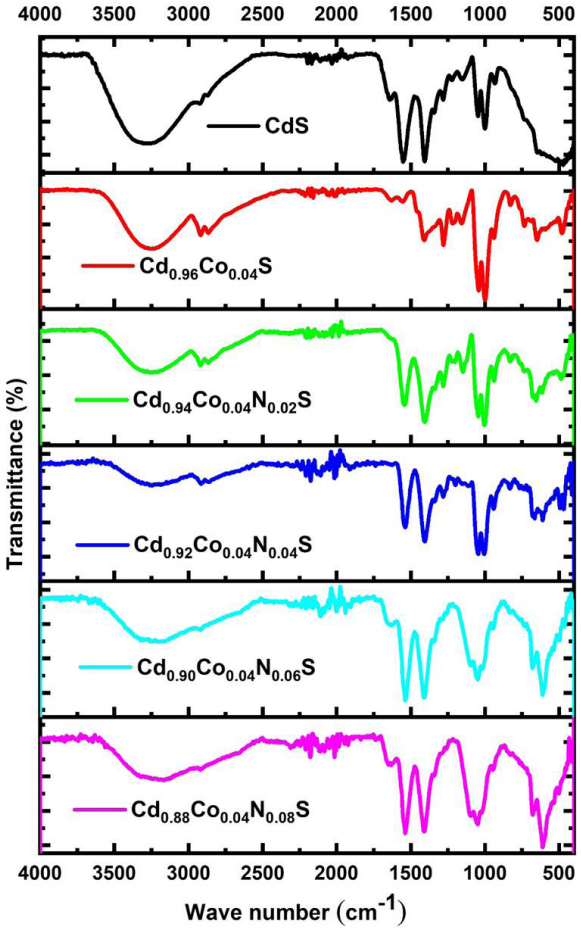


Fig. 2: Fourier transform infrared spectra of CdS and $Cd_{0.96-x}Co_{0.04}N_xS$ nanoparticles (where x = 0, 0.02, 0.04, 0.06, 0.08).

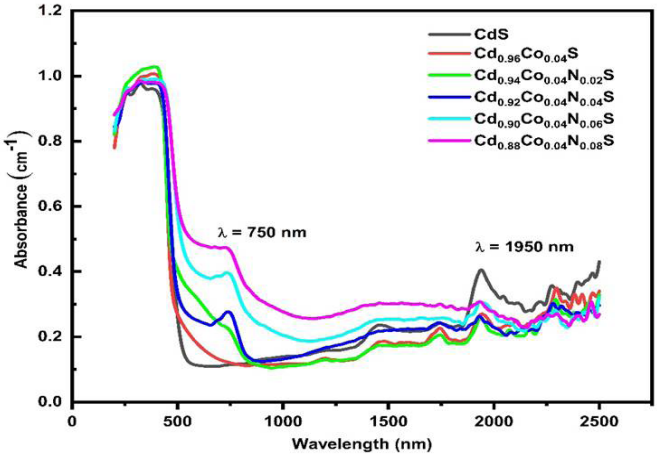


Fig. 3: UV-VIS absorption spectra of the synthesised CdS, and $Cd_{0.96-x}Co_{0.04}N_xS$ nanoparticles (where x = 0, 0.02, 0.04, 0.06, and 0.08).

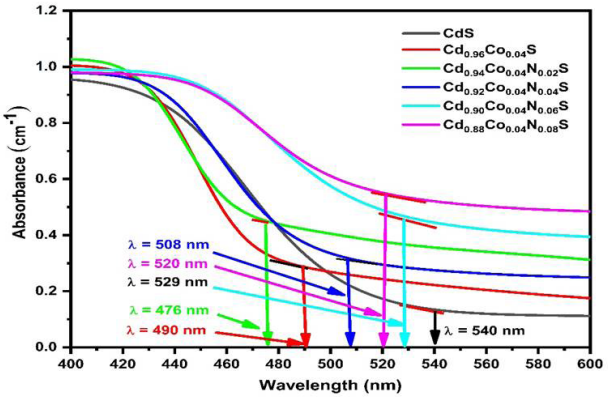


Fig. 4: The absorption band edge positions of CdS and $Cd_{0.96-x}Co_{0.04}N_xS$ nanoparticles (where x = 0, 0.02, 0.04, 0.06, 0.08).

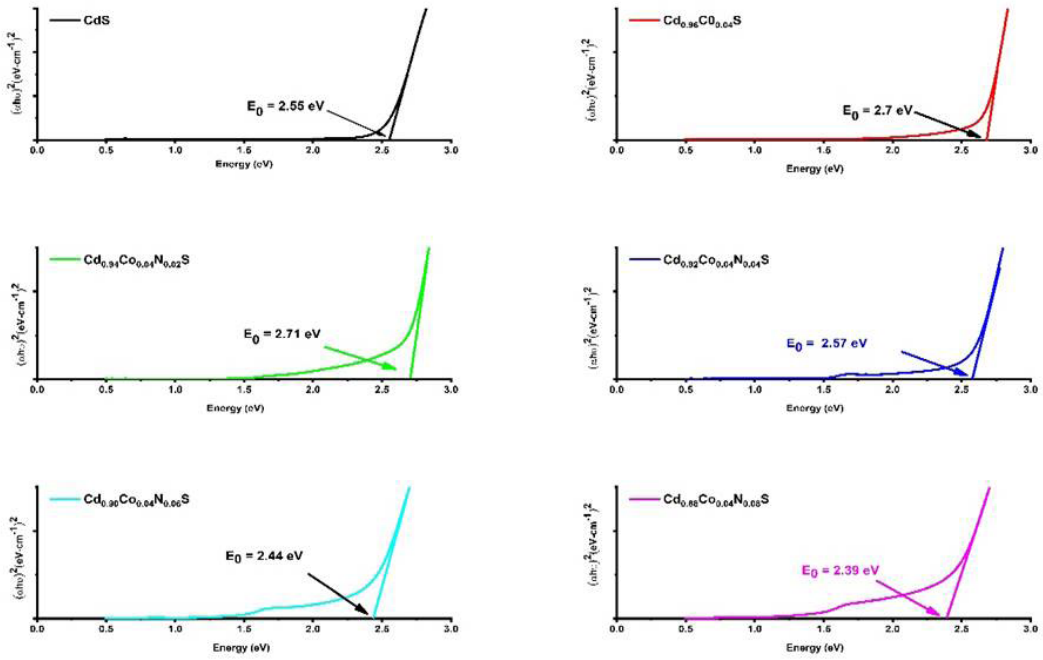


Fig. 5: The Tauc's plots show band gap values of CdS and $Cd_{0.96-x}Co_{0.04}N_xS$ nanoparticles (where x = 0, 0.02, 0.04, 0.06, and 0.08).

UV-VIS spectra band gap

The Tauc's plots of as-prepared nanoparticles are shown in Fig. 5. From the Tauc's plot drawn between the energy hν and $(\alpha h\nu)^2$, where 'ν' is the frequency of the incident light and 'α' is the absorption coefficient of the material, bandgap values are estimated. From Table 2, the intrinsic CdS band gap energy (2.54 eV) is greater than the bulk CdS band gap energy (2.42 eV), which indicates the presence of a quantum confinement effect. With the inclusion of nitrogen, the bandgap value increases from 2.54 eV to 2.70 eV, then decreases to 2.39 eV with increasing cobalt concentration, which is attributed to the Burstein-Mass effect [18]. The redshift in bandgap is observed with an increase in Co^{2+} ion concentration, which could be attributed to d-d exchange interactions between the band electrons in CdS and the localised d electrons of the Co^{2+} ions [19]. The absorption band in Fig. 3 at 750nm confirms the tetrahedral phase of Co^{2+}in as-prepared nanoparticles [20-21]. In this way, the tailoring of the band gap in Co:CdS is possible with N [22].

CONCLUSION

The successful synthesis of nitrogen and cobalt co-doped CdS nanoparticles using a co-precipitation method demonstrates significant modifications in structural, electrical, and optical properties. The incorporation of Co and N into the CdS lattice resulted in reduced crystallite size, increased stability, and tunable lattice strain, as confirmed by XRD and Rietveld analysis. Optical studies revealed adjustable band gaps, attributed to quantum confinement and dopant interactions, enhancing the material's applicability in optoelectronic devices. This research emphasises the potential of co-doped CdS nanoparticles in advanced technologies and provides a basis for further exploration of non-metallic doping strategies in semiconductor materials.

REFERENCES

1. K. A. Bogle, S. Ghosh, S. D. Dhole *et al.*, "Co:CdS diluted magnetic semiconductor nanoparticles: Radiation synthesis, dopant-defect complex formation, and unexpected magnetism," *Chemistry of Materials*, vol. 20, no. 2, pp. 440–446, 2008, doi: 10.1021/cm702118w.
2. S. Muruganandam, G. Anbalagan, and G. Murugadoss, "Optical, electrochemical and thermal properties of Co2+-doped CdS nanoparticles using polyvinylpyrrolidone," *Applied Nanoscience (Switzerland)*, vol. 5, no. 2, pp. 245–253, 2015, doi: 10.1007/s13204-014-0313-6.
3. S. Kumar and J. K. Sharma, "Stable phase CdS nanoparticles for optoelectronics: A study on surface morphology, structural and optical characterisation," *Materials Science- Poland*, vol. 34, no. 2, pp. 368–373, 2016, doi: 10.1515/msp-2016-0033.
4. B. S. Rao, B. R. Kumar, V. R. Reddy, and T. S. Rao, "Preparation and Characterization of Cds Nanoparticles by Chemical Co-precipitation Technique," vol. 8, no. 3, pp. 177–185, 2011.
5. N. H. Patel, M. P. Deshpande, and S. H. Chaki, "Influence of Co-doping on the optical and magnetic properties of CdS nanoparticles," *Journal of Materials Science: Materials in Electronics*, vol. 29, no. 13, pp. 11394–11403, 2018, doi: 10.1007/s10854-018-9230-x.
6. R. Murugesan, S. Sivakumar, K. Karthik, P. Anandan, and M. Haris, "Structural, optical and magnetic behaviors of Fe/Mn-doped and co-doped CdS thin films prepared by spray pyrolysis method," *Appl Phys A Mater Sci Process*, vol. 125, no. 4, 2019, doi: 10.1007/s00339-019-2577-x.
7. M. Elango, D. Nataraj, K. P. Nazeer, and M. Thamilselvan, "Synthesis and characterization of nickel doped cadmium sulfide (CdS : Ni 2 +) nanoparticles," *Mater Res Bull*, vol. 47, no. 6, pp. 1533–1538, 2012, doi: 10.1016/j.materresbull.2012.02.033.
8. G. Murugadoss, "Luminescence properties of co-doped ZnS:Ni, Mn and ZnS:Cu, Cd nanoparticles," *J Lumin*, vol. 132, no. 8, pp. 2043–2048, 2012, doi: 10.1016/j.jlumin.2012.02.011.
9. C. Madhu, A. Sundaresan, and C. N. R. Rao, "Room-temperature ferromagnetism in undoped GaN and CdS semiconductor nanoparticles," *Phys Rev B Condens Matter Mater Phys*, vol. 77, no. 20, pp. 3–6, 2008, doi: 10.1103/PhysRevB.77.201306.
10. P. Kaur, S. Kumar, A. Singh, and S. M. Rao, "Improved magnetism in Cr doped ZnS nanoparticles with nitrogen co-doping synthesized using chemical co-precipitation technique," *Journal of Materials Science: Materials in Electronics*, vol. 26, no. 11, pp. 9158–9163, 2015, doi: 10.1007/s10854-015-3605-z.
11. A. Thesis, F. O. F. Science, and K. Kaur, "Optical and magnetic behaviour of metal doped-CdS nanostructures," no. 901112004, p. 2016, 2016.
12. I. S. Popov, N. S. Kozhevnikova, M. A. Melkozerova, A. S. Vorokh, and A. N. Enyashin, "Nitrogen-doped ZnS nanoparticles: Soft-chemical synthesis, EPR statement and quantum-chemical characterization," *Mater Chem Phys*, vol. 215, pp. 176–182, 2018, doi: 10.1016/j.matchemphys.2018.04.115.
13. M. F. Kotkata, A. E. Masoud, M. B. Mohamed, and E. A. Mahmoud, "Synthesis and structural characterization of CdS nanoparticles," *Physica E Low Dimens Syst Nanostruct*, vol. 41, no. 8, pp. 1457–1465, 2009, doi: 10.1016/j.physe.2009.04.020.
14. P. Chand, R. Ghosh, and Sukriti, "Investigation of structural, morphological and optical properties of Zn doped CdS nanostructures synthesized via co-precipitation method," *Optik (Stuttg)*, vol. 161, pp. 44–53, 2018, doi: 10.1016/j.ijleo.2018.02.031.
15. G. Giribabu, G. Murali, D. Amaranatha Reddy, C. Liu, and R. P. Vijayalakshmi, "Structural, optical and magnetic properties of Co-doped CdS nanoparticles," *J Alloys Compd*, vol. 581, pp. 363–368, 2013, doi: 10.1016/j.jallcom.2013.07.082.
16. P. I. Archer, S. A. Santangelo, and D. R. Gamelin, "Direct observation of sp-d exchange interactions in colloidal Mn 2+ - And Co2+ -doped CdSe quantum dots," *Nano Lett*, vol. 7, no. 4, pp. 1037–1043, Apr. 2007, doi: 10.1021/nl0702362.
17. A. Mesaros *et al.*, "Synthesis, structural and morphological characteristics, magnetic and optical properties of Co-doped ZnO nanoparticles," *Ceram Int*, vol. 40, no. 2, pp. 2835–2846, 2014, doi: 10.1016/j.ceramint.2013.10.030.
18. G. Giribabu, G. Murali, D. Amaranatha Reddy, C. Liu, and R. P. Vijayalakshmi, "Structural, optical and magnetic properties of Co-doped CdS nanoparticles," *J Alloys Compd*, vol. 581, pp. 363–368, 2013, doi: 10.1016/j.jallcom.2013.07.082.
19. N. Jeevanantham and O. N. Balasundaram, "High-performance visible light photocatalytic activity of cobalt (Co) doped CdS nanoparticles by wet chemical route," *Journal of the Iranian Chemical Society*, vol. 16, no. 2, pp. 243–251, 2019, doi: 10.1007/s13738-018-1499-4.
20. G. Giribabu, G. Murali, and R. P. Vijayalakshmi, "Structural, magnetic and optical properties of cobalt and manganese codoped CdS nanoparticles," *Mater Lett*, vol. 117, pp. 298–301, 2014, doi: 10.1016/j.matlet.2013.12.024.
21. G. Giribabu, D. A. Reddy, G. Murali, and R. P. Vijayalakshmi, "Structural and optical studies on Mg-doped CdS nanoparticles by simple co-precipitation method," *AIP Conf Proc*, vol. 1512, pp. 186–187, 2013, doi: 10.1063/1.4790973.
22. X. He and L. Gao, "Morphology and phase evolution of hierarchical architectures of cadmium sulfide," *Journal of Physical Chemistry C*, vol. 113, no. 25, pp. 10981–10989, 2009, doi: 10.1021/jp9026833.